J. Phys. B: At. Mol. Opt. Phys. **41** (2008) 025201 (10pp) doi:10.1088/0953-4075/41/2/025201

Ab initio optical potentials for elastic electron and positron scattering from the heavy noble gases

S Chen[1], R P McEachran[2] and A D Stauffer[1]

[1] Department of Physics and Astronomy, York University, Toronto, Canada, M3J 1P3
[2] Centre for Antimatter-Matter Studies, Research School of Physical Sciences and Engineering, Australian National University, Canberra, ACT 0200, Australia

Received 24 October 2007, in final form 20 November 2007
Published 8 January 2008
Online at stacks.iop.org/JPhysB/41/025201

Abstract
We have derived a non-local, complex and *ab initio* absorption potential within the framework of the relativistic Dirac scattering equations and applied it to elastic scattering of electrons and positrons from the heavy noble gases. We have also developed a perturbation method based on the Hulthén–Kato formalism that enables us to calculate the scattering phase shifts using only real quantities and with a very significant reduction in computational effort. We have used this method to calculate differential cross sections and spin asymmetry parameters for the elastic scattering of electrons from krypton. In addition, we have applied this method to the elastic scattering of positrons from krypton. Our results are compared to experimental measurements and substantial improvements are obtained at intermediate energies with respect to calculations either without an absorption potential or with a semi-empirical absorption potential.

1. Introduction

Below any inelastic scattering thresholds, the scattering of electrons and positrons from atoms can be well represented as a potential scattering problem by including the static and polarization potentials as well as exchange in the case of electrons. Above these thresholds, the existence of additional exit channels for the incident particle flux means that simple potential scattering models produce an overestimate of the elastic cross sections. More elaborate theories, such as the convergent close coupling (Bray and Stelbovics 1992) or *R*-matrix (Burke *et al* 1971) methods, take into account these additional channels but at the cost of a very substantial increase in the complexity of the problem and computer resources needed. A simple way to take into account the open inelastic channels within the framework of a potential scattering problem is to use a complex optical potential where the imaginary part represents the absorption of flux into these channels.

We have previously used such an approach with the non-relativistic Schrödinger equation for the scattering of electrons and positrons from neon and argon (Bartschat *et al* 1988, 1990). We have also included a semi-empirical model absorption potential in the Dirac equations for the scattering of electrons from krypton (McEachran and Stauffer 2003). It is clear that the use of such potentials can substantially improve the accuracy of these scattering calculations.

In this paper we develop a non-local, complex and *ab initio* optical potential based on the Dirac equations which can be improved systematically and then apply it to the scattering of electrons and positrons from krypton. We have previously shown (McEachran and Stauffer 1987) that the use of the Dirac equations to represent both the target states and the free electron can have a substantial effect on the elastic scattering of electrons from the heavy noble gas xenon. Moreover, calculations of spin-dependent quantities such as the Sherman function reported in this paper are most readily represented within the framework of the Dirac equations. As well, the excited states of the heavy noble gases which are required in this work can be best described in j-j coupling which is the natural coupling scheme for the Dirac equations. We note that differential cross sections for electron scattering from xenon using this optical potential have already been published (Cho *et al* 2006). We also derive a method of solving the scattering equations using only real arithmetic by treating the imaginary part of the potential as a perturbation within the Hulthén–Kato formalism.

2. Theory

The noble gases are characterized by having individual electronic excitation cross sections which are small relative to the elastic cross section, although the total excitation cross section can be a significant fraction of the elastic one. However, the ionization cross section is comparable in size to the elastic cross section. Hence, to obtain an accurate absorption potential we must take into account both open excitation and ionization channels. For positronic excitation and ionization the situation is the same except that there is an additional inelastic channel, namely positronium formation. This latter channel is not included in the present formulation of our optical potential. In addition, the wavefunctions for the heavier noble gases, particularly for the excited states, are better described in j-j coupling than LS coupling. This is most readily accomplished by using the Dirac Hamiltonian to represent the target atom instead of the more usual Schrödinger equation.

Our earlier work on optical potentials (Bartschat *et al* 1988, 1990) was based on the work of Bransden and Coleman (1972). The present work differs in two substantial ways from our earlier version: it is developed within the context of the Dirac rather than the Schrödinger formalism and it includes continuum states in the optical potential which our earlier work did not.

We write the wavefunction of the atomic target as Ψ_ν where $\nu = \bar{\nu} J_1 M_1$ is a set of quantum numbers which includes the total angular momentum $J_1 M_1$ while $\bar{\nu}$ represents any other quantum numbers required to specify the target state. These states include both bound excited states as well as continuum states where one of the atomic electrons is free. These latter wavefunctions are included to represent ionization channels. We then introduce the uncoupled channel functions

$$\Psi_\gamma(\boldsymbol{r}, \sigma, \hat{\boldsymbol{x}}, \sigma_x) = \Psi_\nu(\boldsymbol{r}, \sigma)\Theta_{\kappa_2 m_2}(\hat{\boldsymbol{x}}, \sigma_x), \tag{1}$$

where

$$\Theta_{\kappa_2 m_2}(\hat{\boldsymbol{x}}, \sigma_x) = \begin{pmatrix} \chi_{\kappa_2 m_2}(\hat{\boldsymbol{x}}, \sigma_x) & 0 \\ 0 & \chi_{-\kappa_2 m_2}(\hat{\boldsymbol{x}}, \sigma_x) \end{pmatrix} \tag{2}$$

represents the angular momentum and spin functions of the incident particle (electron or positron) and γ is the set of quantum numbers $\nu\kappa_2 m_2$. Here the quantum number κ_2 of the incident particle is related to its total and orbital angular momentum quantum numbers j_2 and l_2 according to $\kappa_2 = -l_2 - 1$ when $j_2 = l_2 + \frac{1}{2}$ and $\kappa_2 = l_2$ when $j_2 = l_2 - \frac{1}{2}$. The individual spin and angular momentum functions are given by

$$\chi_{\kappa m}(\hat{\boldsymbol{r}}, \sigma) = \sum_M C(l\tfrac{1}{2}j; M, m-M) Y_{lM}(\hat{\boldsymbol{r}}) \psi_{\frac{1}{2}, m-M}(\sigma) \tag{3a}$$

$$\chi_{-\kappa m}(\hat{\boldsymbol{r}}, \sigma) = \sum_M C(\bar{l}\tfrac{1}{2}j; M, m-M) Y_{\bar{l}M}(\hat{\boldsymbol{r}}) \psi_{\frac{1}{2}, m-M}(\sigma), \tag{3b}$$

where the Y_{lm} are the usual spherical harmonics and the $\psi_{\frac{1}{2}m}$ are the Pauli spinors. The orbital angular momentum quantum numbers are related by $\bar{l} = 2j - l$. As will be discussed in section 3, the bound atomic states will, in general, be represented by linear combinations of the wavefunctions Ψ_ν.

However, it is the total angular momentum quantum numbers JM of the projectile–atom system which are separately conserved. We therefore construct the coupled channel functions

$$\Psi_\Gamma(\boldsymbol{r}, \sigma, \hat{\boldsymbol{x}}, \sigma_x) = \sum_\gamma (\gamma \mid \Gamma) \Psi_\gamma(\boldsymbol{r}, \sigma, \hat{\boldsymbol{x}}, \sigma_x) \tag{4}$$

which are eigenfunctions of the total angular momentum of the scattering system with quantum numbers JM while the quantum numbers represented by Γ are $\bar{\nu}\kappa_2 JM$. These uncoupled and coupled representations are related by the unitary transformation

$$(\gamma \mid \Gamma') = \delta(\bar{\nu} J_1 \kappa_2, \bar{\nu}' J_1' \kappa_2') C(J_1 j_2 J'; M_1' m_2' M'). \tag{5}$$

We can then write the wavefunction of the target atom plus incident projectile as

$$\Psi(\boldsymbol{r}, \sigma, \boldsymbol{x}, \sigma_x) = \mathcal{A} \sum_\Gamma \Psi_\Gamma(\boldsymbol{r}, \sigma, \hat{\boldsymbol{x}}, \sigma_x) R_\Gamma(x), \tag{6}$$

where the radial function of the projectile is given by

$$R_\Gamma(x) = \frac{1}{x} \begin{pmatrix} F_\Gamma(x) \\ \mathrm{i} G_\Gamma(x) \end{pmatrix} \tag{7}$$

and $\mathcal{A}$ is the antisymmetrization operator which is absent for positron scattering. We note that the expansion (6) includes both a summation over the bound atomic states as well as an integration over the continuum states. The substitution of equation (6) into the Dirac equations for the total system and the subsequent projection onto the channel functions Ψ_Γ yields the following set of close coupling equations:

$$F_\Gamma'(x) + \frac{\kappa_2}{x} F_\Gamma(x) - \frac{1}{\hbar c}[\tilde{\epsilon}_\nu + mc^2] G_\Gamma(x) = -\frac{e^2}{\hbar c} \sum_{\Gamma'} V_{\Gamma\Gamma'}(x) G_{\Gamma'}(x) - \frac{e^2}{\hbar c} \sum_{\Gamma'} W_{\Gamma\Gamma'}(x) G_{\Gamma'}(x) \tag{8a}$$

$$G_\Gamma'(x) - \frac{\kappa_2}{x} G_\Gamma(x) + \frac{1}{\hbar c}[\tilde{\epsilon}_\nu - mc^2] F_\Gamma(x) = +\frac{e^2}{\hbar c} \sum_{\Gamma'} V_{\Gamma\Gamma'}(x) F_{\Gamma'}(x) + \frac{e^2}{\hbar c} \sum_{\Gamma'} W_{\Gamma\Gamma'}(x) F_{\Gamma'}(x) \tag{8b}$$

for the radial functions of the incident particle. Here the direct potentials are

$$V_{\Gamma\Gamma'}(x) = \epsilon \frac{Z}{x} \delta(\Gamma, \Gamma') - \epsilon \bar{V}_{\Gamma\Gamma'}(x) \tag{9}$$

with

$$\bar{V}_{\Gamma\Gamma'}(x) = \sum_{i=1}^{N} \langle \Psi_\Gamma | \frac{1}{|\boldsymbol{r}_i - \boldsymbol{x}|} | \Psi_{\Gamma'} \rangle \tag{10}$$

and for electrons the exchange terms are given by

$$W_{\Gamma\Gamma'}(x) R_{\Gamma'}(x) = \sum_{i=1}^{N} \langle \Psi_\Gamma | \frac{1}{|\boldsymbol{r}_i - \boldsymbol{x}|} | (\mathcal{A} - 1) \{ \Psi_{\Gamma'} R_{\Gamma'} \} \rangle. \tag{11}$$

In equations (8*a*) and (*b*), the parameter $\tilde{\epsilon}_\nu = m\gamma c^2$ is the total relativistic energy of the incident particle while in equation (9), the parameter ϵ is +1 for positrons and −1 for electrons.

We now divide our total scattering space into two parts denoted by P and Q. In our treatment, the P space consists of only the elastic scattering channel while the Q space includes all of the excitation and ionization channels. For the Q space channels we approximate equations (8*a*) and (*b*) by including coupling only to the P space channels (the elastic channel in our case which we now denote by $\Gamma = 0$) as well as by ignoring exchange. This leads to the reduced equations for the Q space:

$$F'_{\Gamma'}(x) + \frac{\kappa'_2}{x} F_{\Gamma'}(x) - \frac{1}{\hbar c}[\tilde{\epsilon}_{\nu'} + mc^2] G_{\Gamma'}(x) = -\frac{e^2}{\hbar c} V_{\Gamma' 0}(x) G_0(x) \tag{12a}$$

$$G'_{\Gamma'}(x) - \frac{\kappa'_2}{x} G_{\Gamma'}(x) + \frac{1}{\hbar c}[\tilde{\epsilon}_{\nu'} - mc^2] F_{\Gamma'}(x) = +\frac{e^2}{\hbar c} V_{\Gamma' 0}(x) F_0(x), \tag{12b}$$

where the parameter $\tilde{\epsilon}_{\nu'}$ is the total relativistic energy of the incident particle when the atom is in the state denoted by ν'. The experimental excitation energies of the atom were used in the determination of these parameters. Equations (12*a*) and (*b*) have a formal solution with outgoing wave boundary conditions, namely

$$\begin{pmatrix} F_{\Gamma'}(x) \\ G_{\Gamma'}(x) \end{pmatrix} = -\frac{1}{k_{\nu'}} \int_0^\infty \mathrm{d}r\, U_{\Gamma' 0}(r) G^Q_{\Gamma'}(x, r) \begin{pmatrix} F_0(r) \\ G_0(r) \end{pmatrix}. \tag{13}$$

Note that in equations (12*a*) and (*b*) we have also ignored the diagonal potential $V_{\Gamma'\Gamma'}$. In principle, we could have retained it but then we would need to have a numerical Green's function in place of the analytic one used here since the potential is in numerical form. We found (Bartschat *et al* 1990) that retaining this diagonal potential made very little difference in the case of neon. The particular form of the Green's function $G^Q_{\Gamma'}(x, r)$ is given in matrix form by

$$G^Q_\Gamma(x, r)_{ij} = \begin{cases} \bar{u}_i(k_{\nu'} x) v_j(k_{\nu'} r) & \text{for} \quad r < x \\ v_i(k_{\nu'} x) \bar{u}_j(k_{\nu'} r) & \text{for} \quad r > x \end{cases} \tag{14}$$

for $i, j = 1, 2$ while

$$v_1(k_{\nu'} x) = \hat{\jmath}_{l'_2}(k_{\nu'} x) \qquad \bar{u}_1(k_{\nu'} x) = \hat{h}_{l'_2}(k_{\nu'} x) \tag{15a, b}$$

$$v_2(k_{\nu'} x) = s_{\kappa'_2} \frac{\hbar c k_{\nu'}}{\tilde{\epsilon}_{\nu'} + mc^2} \hat{\jmath}_{\bar{l}'_2}(k_{\nu'} x)$$

$$\bar{u}_2(k_{\nu'} x) = s_{\kappa'_2} \frac{\hbar c k_{\nu'}}{\tilde{\epsilon}_{\nu'} + mc^2} \hat{h}_{\bar{l}'_2}(k_{\nu'} x) \tag{15c, d}$$

and

$$\hat{h}_{l'_2}(k_{\nu'} x) = -\hat{n}_{l'_2}(k_{\nu'} x) + i \hat{\jmath}_{l'_2}(k_{\nu'} x) \tag{16}$$

is the complex Riccati–Hankel function where $\hat{\jmath}_l$ and $\hat{n}_l$ are the usual real regular and irregular Riccati–Bessel and Riccati–Neumann functions, respectively.

In equations (15*a*, *b*) and (15*c*, *d*), the parameter $s_{\kappa'_2}$ represents the sign of κ'_2. The wavenumber $k_{\nu'}$ of the outgoing particle is related to its total relativistic energy $\tilde{\epsilon}_{\nu'}$ according to

$$k^2_{\nu'} = \frac{1}{\hbar^2 c^2}\left(\tilde{\epsilon}^2_{\nu'} - m^2 c^4\right) = \frac{m^2 c^2}{\hbar^2}(\gamma^2 - 1) \tag{17}$$

while in general, the so-called reduced potentials $U_{\Gamma\Gamma'}(x)$ are defined by

$$U_{\Gamma\Gamma'}(x) = \frac{(1+\gamma) m e^2}{\hbar^2} V_{\Gamma\Gamma'}(x). \tag{18}$$

We can now substitute the solutions (13) into the P space equations. In these equations we neglect the exchange interaction between the P and Q spaces while keeping the direct interaction between these two spaces. This results in equations which only involve the elastic scattering functions F_0 and G_0. We can then convert these equations into the following integral equations by using a Green's function:

$$\begin{pmatrix} F_0(x) \\ G_0(x) \end{pmatrix} = \begin{pmatrix} v_1(k_0 x) \\ v_2(k_0 x) \end{pmatrix} + \frac{1}{k_0} \int_0^x \mathrm{d}r\, G^P_{\Gamma_0}(x, r) \times \left[U_{00}(r) \begin{pmatrix} F_0(r) \\ G_0(r) \end{pmatrix} - \begin{pmatrix} \overline{W}_P(\kappa_2; r) \\ \overline{W}_Q(\kappa_2; r) \end{pmatrix} + U_{\mathrm{opt}}(r) \begin{pmatrix} F_0(r) \\ G_0(r) \end{pmatrix} \right], \tag{19}$$

where the optical potential is given by

$$U_{\mathrm{opt}}(x) \begin{pmatrix} F_0(x) \\ G_0(x) \end{pmatrix} = \left[U^R_{\mathrm{opt}}(x) - \mathrm{i} U^I_{\mathrm{opt}}(x) \right] \begin{pmatrix} F_0(x) \\ G_0(x) \end{pmatrix} \tag{20}$$

with

$$U^R_{\mathrm{opt}}(x) \begin{pmatrix} F_0(x) \\ G_0(x) \end{pmatrix} = -{\sum_{\Gamma'}}' \frac{1}{k_\nu} U_{0\Gamma'}(x) \times \int_0^\infty \mathrm{d}r\, U_{\Gamma' 0}(r) G^{Q,R}_{\Gamma'}(x, r) \begin{pmatrix} F_0(r) \\ G_0(r) \end{pmatrix} \tag{21a}$$

and

$$U^I_{\mathrm{opt}}(x) \begin{pmatrix} F_0(x) \\ G_0(x) \end{pmatrix} = +{\sum_{\Gamma'}}' \frac{1}{k_\nu} U_{0\Gamma'}(x) \times \int_0^\infty \mathrm{d}r\, U_{\Gamma' 0}(r) G^{Q,I}_{\Gamma'}(x, r) \begin{pmatrix} F_0(r) \\ G_0(r) \end{pmatrix} \tag{21b}$$

while the large and small components of the exchange terms, $\overline{W}_P(\kappa_2; x)$ and $\overline{W}_Q(\kappa_2; x)$, are defined by

$$\overline{W}_P(\kappa_2; x) = -\frac{(1+\gamma) m e^2}{\hbar^2} W_{00}(x) F_0(x) \tag{22a}$$

$$\overline{W}_Q(\kappa_2; x) = -\frac{(1+\gamma) m e^2}{\hbar^2} W_{00}(x) G_0(x), \tag{22b}$$

where $W_{00}(x)$ is, in turn, defined in equation (11). The prime on the summation sign in equations (21*a*) and (*b*) indicates that the term $\Gamma = 0$ is to be omitted. Furthermore, the non-local nature of our optical potential is apparent from these equations. The Green's function $G^P_{\Gamma_0}(x, r)$ in equation (19) can be expressed in matrix form according to

$$G^P_\Gamma(x, r)_{ij} = \bar{v}_i(k_0 x) v_j(k_0 r) - v_i(k_0 x) \bar{v}_j(k_0 r) \tag{23}$$

with $i, j = 1, 2$ where the functions $v_{1,2}(k_0 x)$ are defined in equations (15*a*, *b*) while the functions $\bar{v}_{1,2}(k_0 x)$ are given by

$$\bar{v}_1(k_0 x) = \hat{n}_{l_2}(k_0 x) \qquad \bar{v}_2(k_0 x) = s_{\kappa_2} \frac{\hbar c k_0}{\tilde{\epsilon}_0 + mc^2} \hat{n}_{\bar{l}_2}(k_0 x). \tag{24a, b}$$

Furthermore, the Green's functions $G^{Q,R}_{\Gamma'}(x,r)$ and $G^{Q,I}_{\Gamma'}(x,r)$ in equations (21*a*) and (*b*) represent the real and imaginary parts of the Green's function $G^{Q}_{\Gamma'}(x,r)$ defined in equation (14).

The real part of the optical potential represents the polarization of the target atom by the incident projectile while the imaginary part allows flux to be absorbed into the open inelastic channels. In practice, it is often found that the real part of the optical potential does not adequately describe the polarization interaction. This was the case, for example, in the calculations of Bartschat *et al* (1988, 1990) for the elastic scattering of electrons and positrons from neon and argon, although, in neither case, did these authors include continuum states in their optical potential. Under these circumstances, it is better to replace the real part of the optical potential by a local polarization potential $U_{\rm pol}(x)$ and then just treat the absorption processes in a non-local manner. Equation (19) then reduces to

$$\begin{pmatrix} F_0(x) \\ G_0(x) \end{pmatrix} = \begin{pmatrix} v_1(k_0x) \\ v_2(k_0x) \end{pmatrix} + \frac{1}{k_0}\int_0^x \mathrm{d}r\, G^{P}_{\Gamma_0}(x,r) \times \left[U(r)\begin{pmatrix} F_0(r) \\ G_0(r) \end{pmatrix} - \begin{pmatrix} \overline{W}_P(\kappa_2;r) \\ \overline{W}_Q(\kappa_2;r) \end{pmatrix} - \mathrm{i}U^{\rm I}_{\rm opt}(r)\begin{pmatrix} F_0(r) \\ G_0(r) \end{pmatrix}\right], \tag{25}$$

where the local potential $U(r)$ is given by the sum of the static and local polarization potentials i.e.,

$$U(r) = U_{00}(r) + U_{\rm pol}(r). \tag{26}$$

We have followed this procedure here and have replaced the real part of the optical potential by a local polarization potential based upon a polarized-orbital method which included both static and dynamic terms (McEachran and Stauffer, 1990).

2.1. Hulthén–Kato method

Since the optical potential (20) is both non-local and complex, the numerical solution of equation (25) directly would not only involve using complex arithmetic but, as with electron exchange terms, it would involve an iterative process even for positron scattering. In the case where just the electron exchange terms are included, the number of iterations for small values of $|\kappa_2|$ can vary from roughly ten to several hundreds, depending upon the atom and incident particle energy, in order to achieve convergence. As will be shown in section 4, we include over forty excitation and ionization channels in our summation over Γ' in equation (21*b*) for the imaginary part of the optical potential. The evaluation of these terms for every iteration would require extensive amounts of computer time and possibly even require a 'supercomputer'. In order to simplify the calculation, without any significant loss of accuracy (see table 1 in section 4), we have used the Hulthén–Kato method to treat the imaginary absorption potential as a perturbation which allows us to use real arithmetic for the whole calculation and avoid the iterative process for the imaginary part of the optical potential. Such calculations can then be easily carried out on a modern PC.

The Hulthén–Kato identity has been applied to the Dirac scattering equations by Darewych (1999) and Demesie *et al* (2003) but with respect to *local* perturbation terms. The non-local character of the imaginary part of our optical potential gives rise to a somewhat more complicated formalism. We shall therefore give a brief outline of the so-called Hulthén–Kato identity as applied to a non-local potential here. The development of this identity is much easier in terms of the differential equations for the scattering wavefunction rather than the corresponding integral equations (25).

We now let $\bar{F}_0(x)$ and $\bar{G}_0(x)$ be the solutions to the differential equations corresponding to the integral equations (25). Similarly, we let $F_0(x)$ and $G_0(x)$ be the solutions of these same differential equations but with the imaginary part of the optical potential omitted. Furthermore, we shall assume that these solutions vanish at the origin and have been normalized such that

$$\bar{F}_0(x)_{x\to\infty} \sim \sin\left[k_0x - \frac{l_2\pi}{2} + \bar{\delta}_{\kappa_2}(k_0)\right] \tag{27a}$$

$$\bar{G}_0(x)_{x\to\infty} \sim c_{k_0}\cos\left[k_0x - \frac{l_2\pi}{2} + \bar{\delta}_{\kappa_2}(k_0)\right] \tag{27b}$$

and

$$F_0(x)_{x\to\infty} \sim \sin\left[k_0x - \frac{l_2\pi}{2} + \delta_{\kappa_2}(k_0)\right] \tag{28a}$$

$$G_0(x)_{x\to\infty} \sim c_{k_0}\cos\left[k_0x - \frac{l_2\pi}{2} + \delta_{\kappa_2}(k_0)\right], \tag{28b}$$

where c_{k_0} is given by

$$c_{k_0} = \frac{\hbar c k_0}{\tilde{\epsilon}_0 + mc^2}. \tag{29}$$

We note that the wavefunctions $\bar{F}_0(x)$ and $\bar{G}_0(x)$ as well as the phase shift $\bar{\delta}_{\kappa_2}(k_0)$ are complex quantities whereas the wavefunctions $F_0(x)$ and $G_0(x)$ and the phase shift $\delta_{\kappa_2}(k_0)$ are real.

The Hulthén–Kato identity can now be derived by starting with the following identity

$$[\bar{F}_0G_0 - F_0\bar{G}_0]' = \bar{F}_0G_0' + G_0\bar{F}_0' - F_0\bar{G}_0' - \bar{G}_0F_0', \tag{30}$$

where the prime denotes differentiation with respect to x. The right-hand side of equation (30) can be obtained directly from the differential equations for the scattering wavefunctions. Equation (30) is then integrated from zero to infinity and the left-hand side of the resulting equation is evaluated using the above boundary conditions. We then obtain the following result

$$\begin{aligned}\sin\left[\bar{\delta}_{\kappa_2}(k_0) - \delta_{\kappa_2}(k_0)\right] = {} & \mathrm{i}\frac{e^2}{\hbar^2c^2}\frac{\tilde{\epsilon}_0 + mc^2}{k_0}(1+\gamma) \\ & \times {\sum_{\Gamma'}}' \frac{1}{k_{\nu'}}\int_0^\infty \mathrm{d}x \int_0^\infty \mathrm{d}r\{F_0(x)V_{0\Gamma'}(x)V_{\Gamma'0}(r) \\ & \times [v_1(k_{\nu'}x)v_1(k_{\nu'}r)\bar{F}_0(r) + v_1(k_{\nu'}x)v_2(k_{\nu'}r)\bar{G}_0(r)] \\ & + G_0(x)V_{0\Gamma'}(x)V_{\Gamma'0}(r) \\ & \times [v_2(k_{\nu'}x)v_1(k_{\nu'}r)\bar{F}_0(r) + v_2(k_{\nu'}x)v_2(k_{\nu'}r)\bar{G}_0(r)]\}. \end{aligned} \tag{31}$$

In equation (31), the functions $v_{1,2}(k_{\nu'}x)$ are as defined in equations (15*a*, *c*).

So far, the result given in equation (31) is exact. If we now assume that the optical potential terms act as only a small perturbation upon the solutions of equations (25) then we can replace the wavefunctions $\bar{F}_0$ and $\bar{G}_0$ by the wavefunctions F_0 and G_0 respectively in equation (31). The phase shift difference $\bar{\delta}_{\kappa_2}(k_0) - \delta_{\kappa_2}(k_0)$ will then be pure imaginary i.e.,

$$\bar{\delta}_{\kappa_2}(k_0) - \delta_{\kappa_2}(k_0) = \mathrm{i}\gamma_{\kappa_2}(k_0), \tag{32}$$

where $\gamma_{\kappa_2}(k_0)$ is real and positive. In atomic units, it then follows that, to first order in perturbation theory, equation (31) becomes

$$\sinh\left[\gamma_{\kappa_2}(k_0)\right] = \frac{(1+\gamma)^2}{k_0}\left\{ {\sum_{\Gamma_1'}}' \left[I_{\Gamma'}^{(1)}(k_0) + I_{\Gamma'}^{(2)}(k_0)\right]^2 + {\sum_{\Gamma_2'}}' \int_0^{\Delta\epsilon} \mathrm{d}\epsilon' \left[I_{\Gamma'}^{(3)}(\epsilon', k_0) + I_{\Gamma'}^{(4)}(\epsilon', k_0)\right]^2 \right\}, \tag{33}$$

where we have broken the sum into two parts, one over the bound states of the Q space and the other over the continuum states. Here the integrals $I_{\Gamma'}^{(1)}(k_0)$, $I_{\Gamma'}^{(2)}(k_0)$, $I_{\Gamma'}^{(3)}(\epsilon', k_0)$ and $I_{\Gamma'}^{(4)}(\epsilon', k_0)$ are given by

$$I_{\Gamma'}^{(1)}(k_0) = k_{\nu'}^{-\frac{1}{2}} \int_0^\infty \mathrm{d}x\; V_{0\Gamma'}(x) v_1(k_{\nu'}x) F_0(x) \tag{34a}$$

$$I_{\Gamma'}^{(2)}(k_0) = k_{\nu'}^{-\frac{1}{2}} \int_0^\infty \mathrm{d}x\; V_{\Gamma' 0}(x) v_2(k_{\nu'}x) G_0(x) \tag{34b}$$

$$I_{\Gamma'}^{(3)}(\epsilon', k_0) = k_{\nu'}^{-\frac{1}{2}} \int_0^\infty \mathrm{d}x\; V_{0\Gamma'}(\epsilon', x) v_1(k_{\nu'}x) F_0(x) \tag{34c}$$

and

$$I_{\Gamma'}^{(4)}(\epsilon', k_0) = k_{\nu'}^{-\frac{1}{2}} \int_0^\infty \mathrm{d}x\; V_{\Gamma' 0}(\epsilon', x) v_2(k_{\nu'}x) G_0(x). \tag{34d}$$

Furthermore, in equation (33), the upper integration limit $\Delta\epsilon$ is given by $\epsilon_0 - \epsilon_\mathrm{I}$ where ϵ_0 is the relativistic kinetic energy of the incident electron and ϵ_I is the ionization energy of the atomic state ν. In equation (33), the summation variables Γ_1' and Γ_2' are those subsets of the general summation/integration variable Γ' which only include discrete quantum numbers. Here the summation variable Γ_1' pertains to the discrete excited states while Γ_2' pertains to the continuum states. Furthermore, in the notations for the potentials in equations (34*c*) and (*d*), we have explicitly indicated that they depend on the energy of the free electron in the continuum states (see the following section for more details).

Thus, if we calculate $\delta_{\kappa_2}(k_0)$ from the equations for $F_0(x)$ and $G_0(x)$ and then determine $\gamma_{\kappa_2}(k)$ from equation (33), we can obtain an approximation to the complex phase shift $\bar{\delta}_{\kappa_2} = \delta_{\kappa_2} + \mathrm{i}\gamma_{\kappa_2}$ which not only involves calculations with real quantities but also avoids the re-evaluation of the non-local absorption potential in an iterative process. Note that in this approximation, the addition of an imaginary potential does not change the real part of the phase shift.

2.2. Scattering parameters

Once the complex phase shifts $\bar{\delta}_{\kappa_2}$ have been determined from equation (32), the direct and spin-flip scattering amplitudes can be calculated in terms of the T-matrix elements according to

$$f(\theta) = \frac{1}{k_0}\sum_{l_2=0}^{\infty}\left[(l_2+1)T_{l_2}^{+}(k_0) + l_2 T_{l_2}^{-}(k_0)\right]P_{l_2}(\cos\theta) \tag{35a}$$

$$g(\theta) = \frac{1}{k_0}\sum_{l_2=0}^{\infty}\left[T_{l_2}^{-}(k_0) - T_{l_2}^{+}(k_0)\right]P_{l_2}^{1}(\cos\theta), \tag{35b}$$

where $P_{l_2}(\cos\theta)$ and $P_{l_2}^1(\cos\theta)$ are the Legendre and associated Legendre polynomials and

$$T_{l_2}^{\pm}(k_0) = \frac{1}{2\mathrm{i}}\left[\exp\left(2\mathrm{i}\bar{\delta}_{l_2}^{\pm}(k_0)\right) - 1\right]. \tag{36}$$

Here $T_{l_2}^{+}$ is the T-matrix element corresponding to spin-up $\left(\kappa_2 < 0,\, j_2 = l_2 + \frac{1}{2}\right)$ while $T_{l_2}^{-}$ corresponds to spin-down $\left(\kappa_2 > 0,\, j_2 = l_2 - \frac{1}{2}\right)$. In terms of these scattering amplitudes, the differential cross section $\sigma(\theta, \phi)$ is given by

$$\sigma(\theta, \phi) = |f(\theta)|^2 + |g(\theta)|^2 \tag{37}$$

while the Sherman function is given by

$$S(\theta) = \mathrm{i}\frac{f(\theta)g^*(\theta) - f^*(\theta)g(\theta)}{|f(\theta)|^2 + |g(\theta)|^2}. \tag{38}$$

The Sherman function is a measure of the amount of spin polarization produced by scattering from an unpolarized electron beam or equivalently the left–right scattering asymmetry which occurs when the incident electron beam is spin polarized perpendicular to the scattering plane.

In terms of the real and imaginary parts of the phase shifts, the integrated elastic cross section is given by

$$\sigma^{\mathrm{el}}\left(k_0^2\right) = \frac{2\pi}{k_0^2}\sum_{l_2=0}^{\infty}\left\{(l_2+1)\exp\left(-2\gamma_{l_2}^{+}\right)\left[\cosh 2\gamma_{l_2}^{+} - \cos 2\delta_{l_2}^{+}\right] + l_2\exp\left(-2\gamma_{l_2}^{-}\right)\left[\cosh 2\gamma_{l_2}^{-} - \cos 2\delta_{l_2}^{-}\right]\right\} \tag{39}$$

while the total inelastic or absorption cross section is given by

$$\sigma^{\mathrm{inel}}\left(k_0^2\right) = \frac{\pi}{k_0^2}\sum_{l_2=0}^{\infty}\left\{(l_2+1)\left[1 - \exp\left(-4\gamma_{l_2}^{+}\right)\right] + l_2\left[1 - \exp\left(-4\gamma_{l_2}^{-}\right)\right]\right\}. \tag{40}$$

3. Calculations

We have used the GRASP92 program of Parpia *et al* (1996) to calculate the target wavefunctions for the ground and excited states of krypton. The ground state in the P space is represented by a fully varied Dirac–Fock wavefunction with an outer shell $n\bar{\mathrm{p}}^2 n\mathrm{p}^4$ where $\bar{\mathrm{p}}$ represents an electron with total angular momentum $j = \frac{1}{2}$ while p represents an electron with $j = \frac{3}{2}$.

We include in the Q space only those bound and continuum states which have direct matrix elements with the ground state. For the bound states, these have the configuration either $n\bar{\mathrm{p}}n\mathrm{p}^4 m'\kappa'$ or $n\bar{\mathrm{p}}^2 n\mathrm{p}^3 m'\kappa'$ and are calculated in a frozen-core approximation where all of the orbitals except

the valence $n\bar{\mathrm{p}}$ and $n\mathrm{p}$ orbitals and the excited $m'\kappa'$ orbital are kept as calculated for the ground state. In the work presented below, we have chosen κ' to correspond to s, $\bar{\mathrm{p}}$, p, $\bar{\mathrm{d}}$, and d orbitals while m' can be one of $n, n+1$ or $n+2$ respectively. In the case of the noble gases, different atomic configurations can have the same total angular momentum J. Thus, in order to take configuration interaction into account, the atomic wavefunction for a particular excited state of a noble gas is formed by taking a linear combination of the corresponding wavefunctions $\Psi_{\alpha_{\kappa\kappa'' JM}}$ according to the $Jl K$ coupling scheme:

$$\Psi\left(n'\kappa'[K]^P_J\right) = \sum_{\kappa\kappa''} c_{\kappa\kappa''}(n'\kappa' JK)\Psi_{\alpha_{\kappa\kappa'' JM}}, \tag{41}$$

where the expansion coefficients $c_{\kappa\kappa''}(n'\kappa' JK)$ are obtained from the multi-configuration Dirac–Fock calculation. The above summation is not over κ and κ'' separately, but rather over those combinations of κ and κ'' for which the corresponding values of j and j'' will combine to form J. Here κ refers to the core $\bar{\mathrm{p}}$ or p electron which is excited i.e., the various wavefunctions $\Psi_{\alpha_{\kappa\kappa'' JM}}$ in equation (41) will involve both 'cores' while κ'' refers to the electron in an excited state. One of the κ'' values will, of course, be κ'.

With these wavefunctions we can now calculate the direct and exchange potentials for the ground state as well as the coupling potentials. The static potential of the ground state is

$$\begin{aligned} U_{00}(x) &= \frac{(1+\gamma)me^2}{\hbar^2} V_{00}(x) \\ &= \frac{(1+\gamma)me^2}{\hbar^2}\left[\epsilon\frac{Z}{x} - \epsilon\sum_{n\kappa} q_{n\kappa}\frac{1}{x}y_0(n\kappa, n\kappa; x)\right] \end{aligned} \tag{42}$$

while the exchange terms are given by

$$\begin{aligned} \overline{W}_{P\text{ or }Q}(\kappa_2; x) = \frac{(1+\gamma)me^2}{\hbar^2}\sum_{n\kappa}\Bigg\{ &-[\epsilon_{n\kappa}+\epsilon_v]\Delta_{n\kappa_2}\delta(\kappa,\kappa_2) \\ &+ e^2\sum_v q_{n\kappa}\Gamma_{j_2vj}\frac{1}{x}y_v(n\kappa,\kappa_2;x)\Bigg\}\{P_{n\kappa}(x)\text{ or }Q_{n\kappa}(x)\}, \end{aligned} \tag{43}$$

where

$$\frac{1}{x}y_0(n\kappa, n\kappa; x) = \int_0^\infty \mathrm{d}r\ \gamma_0(r,x)\left[P^2_{n\kappa}(r) + Q^2_{n\kappa}(r)\right] \tag{44}$$

while

$$\begin{aligned} \frac{1}{x}y_v(n\kappa,\kappa_2;x) = &\int_0^\infty \mathrm{d}r\ \gamma_v(r,x) \\ &\times\left[P_{n\kappa}(r)F_0(r) + Q_{n\kappa}(r)G_0(r)\right] \end{aligned} \tag{45}$$

and

$$\Delta_{n\kappa_2} = \int_0^\infty \mathrm{d}r[P_{n\kappa}(r)F_0(r) + Q_{n\kappa}(x)G_0(x)]. \tag{46}$$

Here $P_{n\kappa}$ and $Q_{n\kappa}$ are the large and small radial components of the Dirac–Fock orbitals. The coupling potentials $V_{\Gamma'0}(x)$ are given by

$$\begin{aligned} V_{\Gamma'0}(x) = &\epsilon\sum_{\kappa\kappa''} c_{\kappa\kappa''}(n'\kappa' J_1 K) \\ &\times\frac{(-1)^{j+j'_2}}{[(2J_1+1)(2J+1)]^{\frac{1}{2}}} d_{J_1}(\kappa'_2,\kappa_2)d_{J_1}(\kappa'',\kappa) \\ &\times\frac{1}{x}y_{J_1}(n'\kappa'', n\kappa; x)\delta(j_2 JM, JJ'M'), \end{aligned} \tag{47}$$

where the coefficients $d_{J_1}(\kappa',\kappa)$ are defined in terms of the Clebsch–Gordan coefficients according to

$$d_{J_1}(\kappa',\kappa) = \left[\frac{(2j'+1)(2j+1)}{(2J_1+1)}\right]^{\frac{1}{2}} C\left(j' j J_1; \tfrac{1}{2}, -\tfrac{1}{2}\right) \tag{48}$$

and are also subject to the parity constraint that $l'+l-J_1$ must be an even integer. Finally, in equation (43), the coefficient Γ_{j_2vj} is defined by

$$\Gamma_{j_2vj} = \frac{1}{2v+1}C^2\left(j_2 j v; -\frac{1}{2}, \frac{1}{2}\right). \tag{49}$$

We have also included Q space channels which represent ionization. In this case, the $m'\kappa'$ orbital is replaced by a relativistic continuum wavefunction with quantum numbers $\epsilon'\kappa'$ where ϵ' is the relativistic kinetic energy. In the work presented below, we have chosen κ' to correspond to s, $\bar{\mathrm{p}}$, p, $\bar{\mathrm{d}}$, d, $\bar{\mathrm{f}}$, f, $\bar{\mathrm{g}}$ and g waves. We determine these wavefunctions from the integral equations

$$P_{\epsilon'\kappa'}(r) = v^{\mathrm{c}}_1(kr) - \frac{v^{\mathrm{c}}_1(kr)}{k}J_\kappa(r) + \frac{\bar{v}^{\mathrm{c}}_1(kr)}{k}I_\kappa(r) \tag{50a}$$

$$Q_{\epsilon'\kappa'}(r) = v^{\mathrm{c}}_2(kr) - \frac{v^{\mathrm{c}}_2(kr)}{k}J_\kappa(r) + \frac{\bar{v}^{\mathrm{c}}_2(kr)}{k}I_\kappa(r), \tag{50b}$$

which are expressed in terms of the regular and irregular relativistic Coulomb functions. Here the integrals $I_\kappa(r)$ and $J_\kappa(r)$ are defined according to

$$\begin{aligned} I_\kappa(r) = &\int_0^r \mathrm{d}r' \\ &\times\left[v^{\mathrm{c}}_1(kr')U_{\mathrm{c}}(r')P_{\epsilon'\kappa'}(r') + v^{\mathrm{c}}_2(kr')U_{\mathrm{c}}(r')Q_{\epsilon'\kappa'}(r')\right] \end{aligned} \tag{51a}$$

and

$$\begin{aligned} J_\kappa(r) = &\int_0^r \mathrm{d}r' \\ &\times\left[\bar{v}^{\mathrm{c}}_1(kr')U_{\mathrm{c}}(r')P_{\epsilon'\kappa'}(r') + \bar{v}^{\mathrm{c}}_2(kr')U_{\mathrm{c}}(r')Q_{\epsilon'\kappa'}(r')\right]. \end{aligned} \tag{51b}$$

In equations (50*a*) and (*b*), the potential $U_{\mathrm{c}}(r)$ is related to the static potential of the ion core $V_{\mathrm{c}}(r)$ according to

$$U_{\mathrm{c}}(r) = \frac{(1+\gamma)me^2}{\hbar^2}V_{\mathrm{c}}(r), \tag{52}$$

where the potential $V_{\mathrm{c}}(r)$ is given by

$$\begin{aligned} V_{\mathrm{c}}(r) = &-\frac{Z-1}{r} \\ &+\sum_{n\kappa} q_{n\kappa}\frac{1}{r}y_0(n\kappa, n\kappa; r) + \frac{1}{r}y_0(m'\bar{\mathrm{p}}, m'\bar{\mathrm{p}}; r) \end{aligned} \tag{53a}$$

when a $\bar{\mathrm{p}}$ electron is ionized or by

$$\begin{aligned} V_{\mathrm{c}}(r) = &-\frac{Z-1}{r} + \sum_{n\kappa} q_{n\kappa}\frac{1}{r}y_0(n\kappa, n\kappa; r) \\ &+\frac{3}{r}y_0(m'\mathrm{p}, m'\mathrm{p}; r) - 4\Gamma_{j2j}\frac{1}{r}y_2(m'\mathrm{p}, m'\mathrm{p}; r) \end{aligned} \tag{53b}$$

when a p electron is ionized. Here m' represents the principle quantum number of the incomplete subshell while the summation over $n\kappa$ is over all the remaining complete subshells. Furthermore, the coefficient Γ_{j2j} is given by equation (49) with $j = \frac{3}{2}$. We note that the exchange terms in equations (50*a*) and (*b*) for the continuum wavefunctions

Table 1. A comparison of the imaginary part of the phase shift (γ_{κ_2}) calculated exactly and by the Hulthén–Kato method. Also included are the corresponding values of the excitation cross section ($\sigma^{\rm ex}$).

	30 eV		50 eV		60 eV		100 eV	
κ_2	H–K	Exact	H–K	Exact	H–K	Exact	H–K	Exact
−1	0.028 856	0.028 971	0.022 758	0.022 960	0.016 130	0.016 253	0.002 220	0.002 176
−2	0.012 644	0.011 979	0.021 017	0.021 315	0.021 824	0.022 235	0.015 341	0.015 550
1	0.011 757	0.011 202	0.020 186	0.020 471	0.021 363	0.021 740	0.015 801	0.016 052
−3	0.012 504	0.012 994	0.017 865	0.018 460	0.018 374	0.018 951	0.016 641	0.017 136
2	0.012 370	0.012 853	0.017 677	0.018 269	0.018 209	0.018 795	0.016 598	0.017 097
−4	0.022 247	0.022 703	0.020 797	0.021 118	0.019 659	0.019 896	0.014 983	0.015 056
3	0.022 293	0.022 742	0.020 800	0.021 121	0.019 656	0.019 892	0.014 980	0.015 053
−5	0.021 942	0.022 079	0.022 346	0.022 540	0.020 735	0.020 918	0.015 862	0.015 964
4	0.021 953	0.022 086	0.022 354	0.022 545	0.020 740	0.020 922	0.015 863	0.015 965
−6	0.015 717	0.015 751	0.020 544	0.020 625	0.019 675	0.019 764	0.014 521	0.014 591
5	0.015 719	0.015 752	0.020 547	0.020 627	0.019 677	0.019 765	0.014 521	0.014 592
−7	0.009 964	0.009 972	0.017 277	0.017 307	0.017 607	0.017 646	0.014 113	0.014 156
6	0.009 965	0.009 972	0.017 278	0.017 307	0.017 608	0.017 646	0.014 114	0.014 156
−8	0.005 915	0.005 916	0.013 569	0.013 579	0.014 818	0.014 833	0.013 570	0.013 594
7	0.005 915	0.005 916	0.013 569	0.013 579	0.014 819	0.014 833	0.013 571	0.013 594
$\sigma^{\rm ex}\left(k_0^2\right)$	5.708 46	5.737 57	6.608 80	6.638 77	6.442 54	6.467 21	5.359 46	5.370 18

have been omitted. Furthermore, the normalization of the continuum wavefunctions $P_{\epsilon'\kappa'}(r)$ and $Q_{\epsilon'\kappa'}(r)$ is such that

$$\int_0^\infty {\rm d}r[P_{\epsilon\kappa'}(r)P_{\epsilon'\kappa'}(r) + Q_{\epsilon\kappa'}(r)Q_{\epsilon'\kappa'}(r)] = \delta(\epsilon - \epsilon'). \quad (54)$$

For the continuum states, it is not necessary to consider configuration interaction and the coupling potentials simply become

$$V_{\Gamma'0}(\epsilon', x) = \epsilon \frac{(-1)^{j+j_2'}}{[(2J_1+1)(2J+1)]^{\frac{1}{2}}} d_{J_1}(\kappa_2', \kappa_2) d_{J_1}(\kappa', \kappa) \times \frac{1}{x} y_{J_1}(\epsilon'\kappa', n\kappa; x)\delta(j_2 J M, J J' M'). \quad (55)$$

Equation (31) for the imaginary part of the phase shift includes an energy integration over the continuum waves. We have replaced this integration by a Gauss–Legendre quadrature and thus we need to calculate the Coulomb waves for energies specified by the quadrature points.

4. Results

In terms of the intermediate coupling scheme, we have included the following 26 excited states of krypton in our absorption potential, namely, $n'{\rm s}[1/2]_1^{\rm o}$, $n'{\rm s}[3/2]_1^{\rm o}$, $n'\bar{\rm p}[1/2]_0$, $n'\bar{\rm p}[3/2]_2$, $n'{\rm p}[1/2]_0$, $n'{\rm p}[3/2]_2$, $n'{\rm p}[5/2]_2$, $n'\bar{\rm d}[1/2]_1^{\rm o}$, $n'\bar{\rm d}[3/2]_1^{\rm o}$, $n'\bar{\rm d}[5/2]_3^{\rm o}$, $n'{\rm d}[3/2]_1^{\rm o}$, $n'{\rm d}[5/2]_3^{\rm o}$ and $n'{\rm d}[7/2]_2^{\rm o}$ with n' being given by 5 and 6 for s, $\bar{\rm p}$ and p states and by 4 and 5 for the $\bar{\rm d}$ and d states. Note that the parity condition attached to the coefficient defined in equation (48) requires J_1 to be even for states of even parity and odd for states of odd parity in order to have a nonzero direct coupling potential $V_{\Gamma'0}$. In addition, the absorption potential contained the continuum states corresponding to the 13 states listed above but with n' above being replaced by ϵ' plus 12 more states corresponding to $\bar{\rm f}$, f, $\bar{\rm g}$ and g continuum waves. With the inclusion of these excited and continuum states, the total inelastic cross section converged to approximately 3 to 4 significant figures. In the case of the continuum states four Gaussian integration points were found to be sufficient.

As was mentioned in section 2 the real part of the optical potential was replaced with our polarized-orbital polarization potential. In particular, this potential contained the usual polarization multipoles from $\nu = 0$ to 7 as well as dynamic distortion terms for $\nu = 0$ to 6 and is same polarization potential as used by McEachran and Stauffer (2003) in their previous work on krypton.

In table 1 we compare the scattering phase shifts calculated directly from equation (25) with those obtained using the Hulthén–Kato approximation when the 26 discrete excitation channels are included in the absorption potential. We see that the relative error is generally less than 1% but can go as high as 5%. However, the absolute error in the splitting between the spin-up and spin-down phase shifts is much less than the error in the phase shifts themselves. This is particularly important in obtaining accurate values for the spin-flip amplitude and spin-dependent parameters such as the spin asymmetry. The errors decrease as the energy increases and as the angular momentum increases. The last line of the table gives the total excitation cross section as calculated from our phase shifts for $-30 \leqslant \kappa_2 \leqslant 29$. Here the relative error is of the order of 0.5% which is an indication of the error in the scattering parameters which occurs from the use of the Hulthén–Kato approximation. In the determination of the excitation cross section, we used the experimental rather than the theoretical energy differences.

In figure 1 we show our results for the differential cross section for the elastic scattering of electrons from krypton at 20, 30, 50 and 100 eV calculated both with and without the imaginary absorption potential $U_{\rm opt}^I$. These are compared with the experimental measurements of Cho *et al* (2004), Danjo (1988) and Srivastava *et al* (1981). Similar calculations using a semi-empirical absorption potential were published in McEachran and Stauffer (2003) and Cho *et al* (2004).

As expected, the inclusion of an absorption potential reduces the cross section over much of the range of scattering angles, though it does not alter substantially the overall shape of the cross section, and brings it into much better agreement

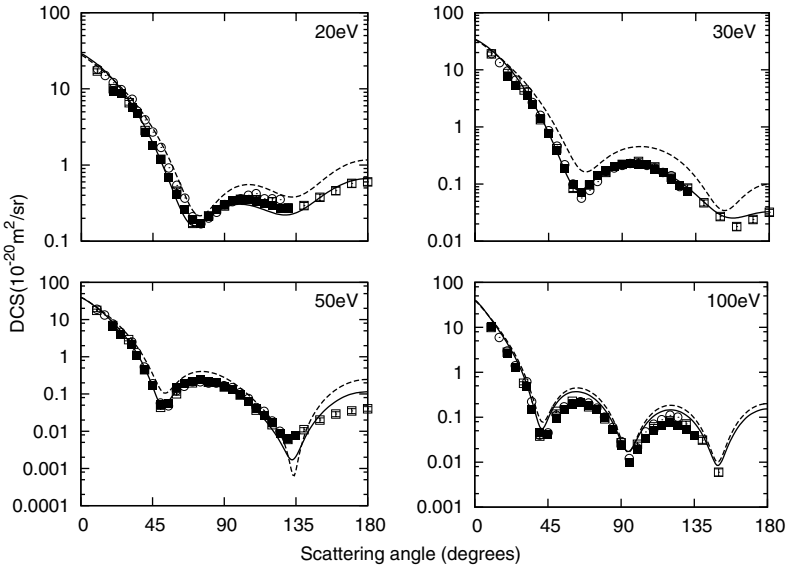

Figure 1. Differential cross sections for the elastic scattering of electrons from krypton at 20, 30, 50 and 100 eV: solid curve, present results including absorption; dashed curve, present results with no absorption. Experimental results: open squares, Cho *et al* (2004); open circles, Danjo (1988); filled squares, Srivastava *et al* (1981).

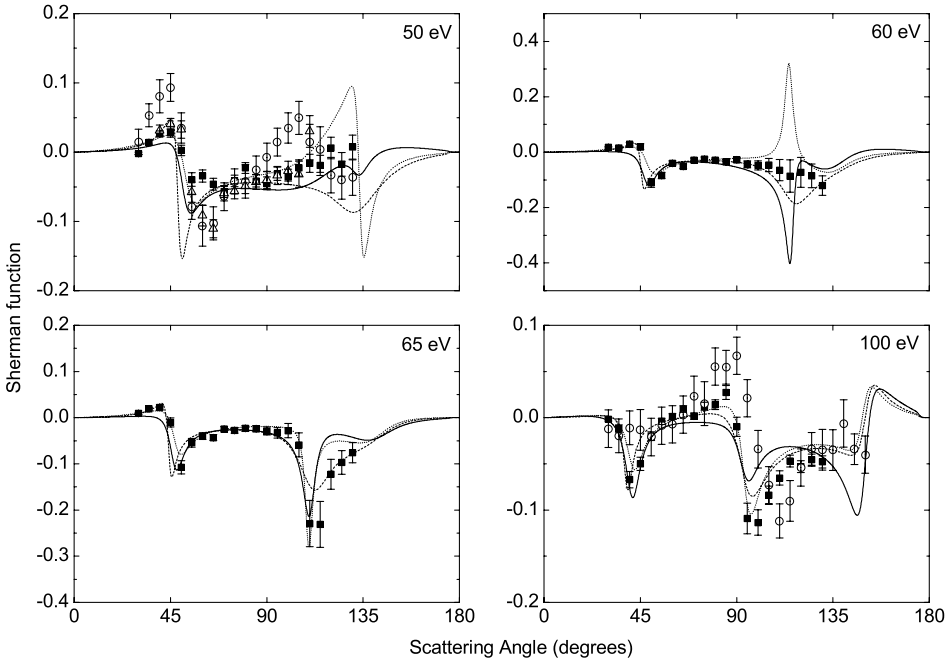

Figure 2. Spin asymmetry for the scattering of spin-polarized electrons from krypton at 50, 60, 65 and 100 eV: solid curve, presents results including absorption; dotted curve, presents results with no absorption, dashed curve, results including semi-empirical absorption, Went *et al* 2002. Experimental results: open triangles, Beerlage *et al* (1981); open circles, Schackert (1968); closed squares, Went *et al* (2002).

with the experimental results. This is particularly important at intermediate angles where, without absorption, our results are considerably larger than experimental measurements. In general, our *ab initio* results are an improvement over the previous calculations using the semi-empirical absorption potential. This is particularly true in the backward direction at 30 eV where the semi-empirical absorption potential yielded results which were approximately a factor of 3 too low. However, at 100 eV the advantage is not so obvious and may indicate the need to include ionization from inner shells in our Q space.

In figure 2 we show our results for the spin asymmetry parameter for the elastic scattering of spin-polarized electrons from krypton atoms which are compared with the experimental results of Beerlage *et al* (1981), Schackert (1968) and Went *et al* (2002). Beerlage *et al* and Schackert measured the spin

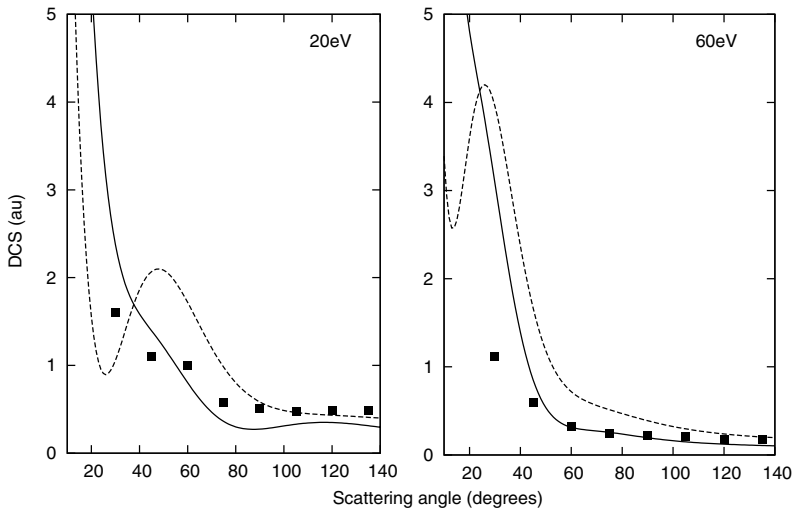

Figure 3. Differential cross sections for the elastic scattering of positrons from krypton at 20 and 60 eV: solid curve, presents results including absorption; dashed curve, presents results with no absorption. Experimental results: open squares, Kauppila *et al* (1996).

polarization of an initially unpolarized electron beam after scattering while Went *et al* used a spin-polarized incident beam and measured the left–right scattering asymmetry. As noted above, the asymmetry parameter measured by these two methods are identical for elastic scattering. Since this parameter varies rapidly for angles near the minima in the differential cross section and the greatest differences among the three approximations as well as with the experimental measurements occur in these regions, we have convoluted our theoretical results with the angular resolution (6.5°) of the experiment of Went *et al* (2002). The effect of the absorption potential is appreciable only in these regions as well. At other angles, there is much better agreement with experiment for all the theoretical results. Given the variation among the experimental measurements at 50 and 100 eV it is difficult to assess the accuracy of our various approximations from the experimental data for this parameter. However, at 50 eV our Sherman function determined with the *ab initio* absorption potential is in much better agreement with experiment at large scattering angles than either our calculation without absorption or with a semi-empirical absorption potential.

Results for the differential cross sections for elastic scattering of positrons from krypton are shown in figure 3 at 20 and 60 eV. We compare our calculations with and without absorption with the experimental measurements of Kauppila *et al* (1996). Most striking is the change in shape of our cross sections when absorption is included in the calculations. This causes the minimum in the cross sections around 20° to disappear completely, in agreement with the measurements, especially at 20 eV. While the range of scattering angles is limited in the measurements of Kauppila *et al* (1996) the disappearance of the minimum at energies above the excitation thresholds is a consistent pattern in all the noble gases. On the other hand, measurements below any inelastic thresholds do show this minimum in agreement with our low energy calculations without absorption (Kauppila *et al* 1996). Thus the inclusion of absorption is vital to obtain the correct shape of the differential cross sections for positron scattering.

5. Conclusions

We have presented our theoretical method, based upon the Dirac equations, for the calculation of an *ab initio* non-local optical potential which accounts for the open inelastic channels for elastic scattering of electrons and positrons from atomic systems at energies above the inelastic thresholds. The real part of this potential represents the polarization of the atomic target during scattering and is calculated by our polarized-orbital method. The imaginary part represents the loss of incident flux into the open inelastic channels and this potential is the main focus of the present work. Besides having no empirical parameters, this method is capable of systematic improvement by including additional states in the Q-space. We have also developed a perturbative approach based on the Hulthén–Kato formalism for solving the scattering equations which does not require the use of complex arithmetic.

This paper also contains detailed formula for scattering from the heavy noble gases and presents results for the elastic scattering of electrons and positrons from krypton atoms at intermediate energies. Our results are compared with experimental measurements for the differential cross section for both electron and positron scattering as well as the spin asymmetry (Sherman) function for electron scattering. The inclusion of the imaginary (absorption) part of the potential reduces the peaks in the differential cross section for electron scattering and results in much improved agreement with experimental data at intermediate and large scattering angles. For positron scattering, the absorption potential substantially changes the shape of the differential cross section in agreement with the pattern of behaviour noted in the experimental measurements. The advantage of using an optical potential for calculating the Sherman function are less obvious due in part to the amount of scatter among the various measurements. Our previously published results for electron scattering from xenon (Cho *et al* 2006) provide further evidence for these conclusions.

Thus we have established the need to include absorption in order to obtain accurate values for the differential cross sections for both electron and positron scattering at intermediate energies and provided an effective, parameter-free method for carrying out these calculations within a potential scattering model. Since this method is based on the Dirac equations it is particularly well suited for scattering from heavy atomic systems such as krypton and xenon.

Acknowledgments

We wish to thank Dr Michael Went for convoluting our theoretical results with his experimental angular resolution and for producing figure 2. This research was supported in part by NSERC Canada.

References

Bartschat K, McEachran R P and Stauffer A D 1988 *J. Phys. B: At. Mol. Opt. Phys.* **21** 2789
Bartschat K, McEachran R P and Stauffer A D 1990 *J. Phys. B: At. Mol. Opt. Phys.* **23** 2349
Beerlage M J M, Zhou Q and Van der Wiel M J 1981 *J. Phys. B: At. Mol. Phys.* **14** 4627
Bransden B and Coleman J P 1972 *J. Phys. B: At. Mol. Phys.* **5** 537
Bray I and Stelbovics 1992 *Phys. Rev.* A **46** 6995
Burke P G, Hibbert A and Robb W D 1971 *J. Phys. B: At. Mol. Phys.* **4** 153
Cho H, McEachran R P, Buckman S J, Filipović, Pejev V, Marinković B P, Tanaka H, Stauffer A D and Jung E C 2006 *J. Phys. B: At. Mol. Opt. Phys.* **39** 3781
Cho H, McEachran R P, Tanaka H and Buckman S J 2004 *J. Phys. B: At. Mol. Opt. Phys.* **37** 4639
Darewych J W 1999 *Phys. Rev.* A **60** 290
Danjo A 1988 *J. Phys. B: At. Mol. Opt. Phys.* **21** 3759
Demesie Amare M, Darewych J W, McEachran R P and Stauffer A D 2003 *J. Phys. B: At. Mol. Opt. Phys.* **36** 665
Kauppila W E, Kwan C K, Przyby D, Smith S J and Stein T S 1996 *Can. J. Phys.* **74** 474
McEachran R P and Stauffer A D 1987 *J. Phys. B: At. Mol. Phys.* **20** 3483
McEachran R P and Stauffer A D 1990 *J. Phys. B: At. Mol. Opt. Phys.* **23** 4605
McEachran R P and Stauffer A D 2003 *J. Phys. B: At. Mol. Opt. Phys.* **36** 3977
Parpia F A, Froese Fischer C and Grant I P 1996 *Comput. Phys. Commun.* **94** 249
Schackert K 1968 *Z. Phys.* **213** 316
Srivastava S K, Tanaka H, Chutjian A and Trajmar S 1981 *Phys. Rev.* A **23** 2156
Went M R, McEachran R P, Lohmann B and MacGillivray W R 2002 *J. Phys. B: At. Mol. Opt. Phys.* **35** 4885